Modeling of rocks under direct shear loading by using discrete element method

1 author:

A. K. Alzo'ubi
Abu Dhabi University

AHU *J. of Engineering & Applied Sciences* 4 (2) 2012

MODELING OF ROCKS UNDER DIRECT SHEAR LOADING BY USING DISCRETE ELEMENT METHOD

A.K. Alzo'ubi.
Department of Civil Engineering, CECS, Abu Dhabi University, P.O.Box 1790, Al Ain, UAE
Email: abdel.alzoubi@adu.ac.ae

ABSTRACT: The geometrical properties are of great concern in characterizing a rock mass. The blocks in a rock mass are formed by flaws with different patterns formed in nature under different geological circumstances. One of the block tessellation models is the Voronoi tessellation, which can be utilized in the discrete element method and used to create realistic rock mass simulation this approach is called UDEC-DM. The UDEC-DM approach has been implemented to model experimental direct shear tests and the results were in good agreement. The effect of degree of persistency of joints inside a direct shear sample was modeled numerically and compared to the behaviour of intact rock. Both closed and opened joints models showed a good agreement with the laboratory results.

***KEYWORDS*:** Numerical Analysis, Tensile Failure, Discrete Element, and Direct Shear

1. INTRODUCTION

Many numerical analysis approaches have been developed in the geotechnical engineering domain, for example: limit equilibrium, discontinuum, continuum, and hybrid methods. Stead et al. [1] presented many of these methods and their disadvantages and advantages; in particular the use of hybrid techniques such as the modeling approach presented in this paper is promising and can handle fracturing of rock masses.

Cundall [2] proposed the discrete element numerical modeling method to allow for the finite displacement and rotations of discrete deformable or rigid blocks, as well as for complete detachment. In the discrete element method, a rock mass is represented as discrete blocks, and discontinuities are treated as interfaces between bodies. The contact displacements and forces at the interfaces are calculated by tracing the movements of the blocks. Applied loads or forces to a block system can cause disturbances that propagate and result in movements. The propagation speed in this dynamic process depends on the physical properties of the blocks and the contacts [3]. The behaviour of the solid material and the discontinuities must be considered.

A time-stepping algorithm must be used to represent the dynamic behaviour, and within a time-step, the velocities and accelerations are assumed to be constant. The time-step is small enough to prevent the propagation of disturbances between one block and its neighbors. This explicit time marching solution scheme is identical to that used by the explicit finite difference method for continuum analysis. The time-step restriction applies to both blocks and contacts as follows. For deformable blocks, the size of the zone is used, and the stiffness of the system includes contributions from both the intact rock modulus and the stiffness at the contacts. For rigid blocks, the block mass and interface stiffness between blocks define the time-step limitation.

The discrete element method calculation step alternates between application of a force displacement law at the contacts and application of Newton's second law at all blocks. Local and global damping is necessary to keep the model under control. This logic is used by the Universal Distinct Element Code (UDEC) [3].

In UDEC, a rock joint is represented numerically as a contact surface formed between two block edges. In general, to detect and identify a contact, for each pair of blocks that touch (or is separated by a small enough gap), data elements are created to represent the point contacts. The adjacent blocks can touch along a common edge segment or at discrete points where a corner meets an edge or another corner (Itasca, [3]). Thus, the number of contact points is increased as a function of the blocks, thereby in-creasing the cycle time. A number of different constitutive models can be applied to the contacts and the solids, such as the Mohr Coulomb failure criterion, which is one of the most acceptable failure criterion in rock mechanics (Figure 1).

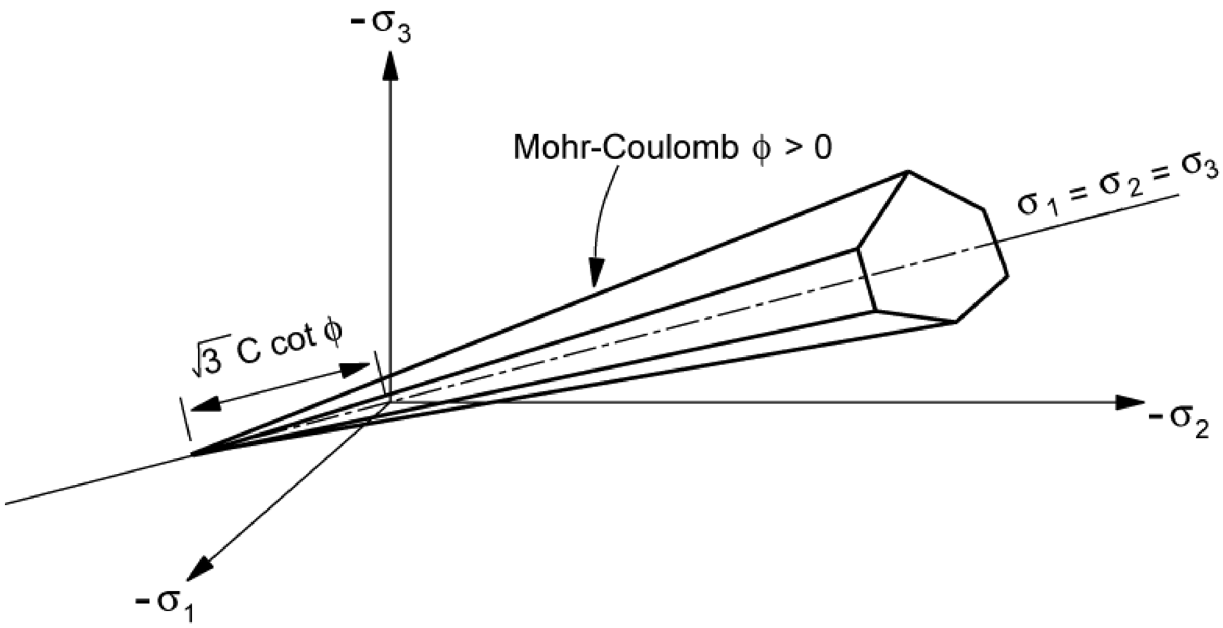

Figure 1: Mohr-Coulomb surface in principal space

Pierce et al. [4] introduced a synthetic rock mass model to simulate jointed rocks that contain joints; this model is also capable of modeling discrete fractures and rupturing inside the rock mass. In their model rounded shaped particles were used which is rarely the case of rock masses.

2. DAMAGE MODEL

The progressive failure of geo-materials is a gradual and time-dependent failure process at localized areas, followed by the redistribution of the stresses in the slope. These new stresses build up and cause the propagation of the failure. If this fracturing continues, a rupture surface connecting all the failed parts will form. Many factors can cause progressive failure, such as the time-dependent degradation of the strength parameters, increasing pore pressures, and/or thermal stresses. In addition, the presence of non-persistent joints and the heterogeneity of the rock mass might cause tensile stresses inside the rock mass and also the initiation and propagation of cracks that might lead to failure. Figure 2 presents a conceptual diagram of the tensile stresses resulting from the compression forces in a block assembly. Cho et al. [5] showed that the development of the through-going rupture surface through intact material is preceded by tensile fracturing.

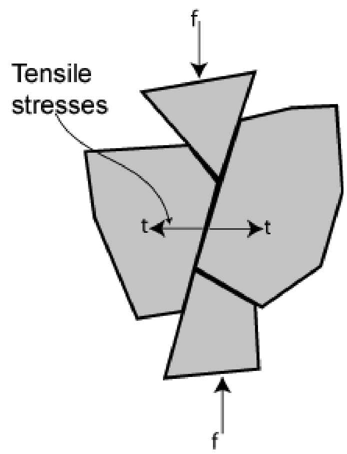

Figure 2: Block assembly subjected to compression forces and the resulting tensile stresses at the bond (Modified from Potyondy and Cundall, [6]

To simulate the rock failure processes by using discrete element modeling, a polygonal block component is added to the usual capability of UDEC [3] to model discrete fractures by using the Voronoi tessellation generator command, which creates randomly sized polygonal blocks. The Voronoi tessellation creates random points within the specified region. Points are also distributed uniformly along each edge. The position of interior points may be relaxed by iteration to create more uniform block distribution. The line segments forming the Voronoi polygons are then generated by constructing perpendicular bisectors of all triangles which share a common side.

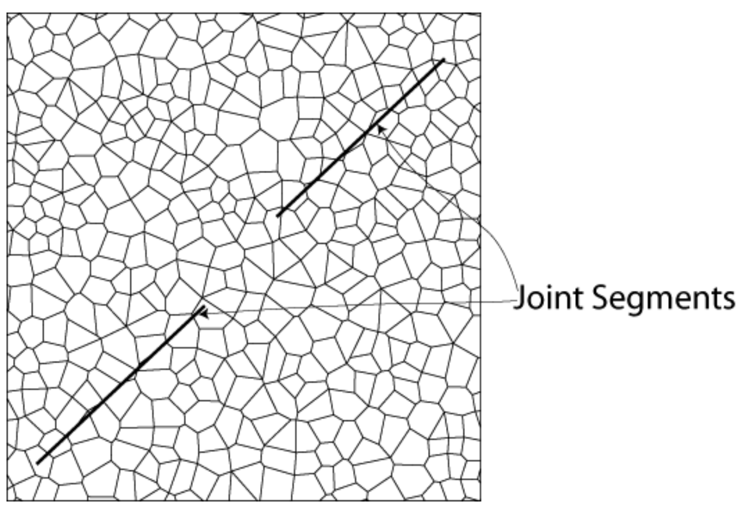

Figure 3: Illustration of the polygonal structure used to simulate blocky intact rock using 100 iterations to generate the flaws.

The randomly sized polygons are analogous to the flaws in the intact rock that can represent grain-boundary flaws or larger-scale internal flaws (Figure 3). The size, seed and number of iterations can be varied to generate randomly sized blocks. For example decreasing the number of iterations to generate the blocks in Figure 3 will result in less uniform blocks. These flaws are defined such that they have intact rock properties and do not contribute additional jointing to the joint system of the rock mass. It should be noted that the term “Damage” is used to describe fracturing of flaws and joint, not plasticity damage.

Lorig and Cundall [7] introduced the Voronoi tessellation to model a concrete member as assemblage of blocks bonded at common boundaries. Failure is simulated by progressive breakage of bonds, Lorig and Cundall's [7] simulation showed the ability to visualize deformed shape and crack development with displacement. Watson et al. [8] used the Voronoi joint to simulate material flow toward dam reservoir in the Checkerboard Creek rock slope, British Columbia, Canada.

Alzo'ubi et al. [9] used this approach to model rock slopes that include persistent and non-persistent smooth rock joints. This polygonal block model will be referred to as the UDEC damage model (UDEC-DM) in this paper. This polygonal block pattern provides a unique method for simulating tensile and/or shear fracturing through intact rock. As they add a new degree of freedom in the model that allows for development of non-directional rupture surface or localized fracturing [7], [10]. Cohesion, friction, and tensile strength can be assigned to the boundaries of these polygonal blocks such that the strength is the same as that of intact rock. Local variation in strength and stiffness can also be applied if required, to simulate any anisotropy in the rock mass such as rocks in sedimentary rocks susceptible to toppling [11].

While the polygonal flaw structure shown in Figure 3 may represent the flaws found in crystalline rocks, these discontinuities are not commonly observed in sedimentary rocks. For sedimentary rocks, the main set of joints should be generated first and then the flaws generated next inside the major bedding units this would simulate the anisotropic rock masses. This approach produces polygonal shapes that are more representative of the cross-cutting joints observed in sedimentary rock than other shapes. Hence, in the UDEC-DM, the user has control over the creation of the internal flaws to match the geological conditions of the rock mass being analyzed.

The blocks created in this approach assigned the elastic, isotropic model of material behaviour. This model exhibits linear stress-strain behaviour with reversible deformations upon unloading. In this model, the relation of stress to strain in increments is expressed by Hookes law. The blocks can be attached together by specifying the friction, cohesion, and tensile bond strength. The boundaries of the blocks were assigned a Mohr-Coloumb criterion that allows slippage and irreversible deformation. The values assigned to these strengths influence the strength of the synthetic rock and the nature of cracking and failure. Once the shear stresses exceed the strength, the shear strength is set to its residual value as long as blocks stay in contact, which is a function of compressive normal stress and the friction angle at the contact. However, once a tensile bond fails the tensile strength of the contact is set to zero.

This flaw pattern provides an extra degree of freedom that is useful to simulate the fracturing of the rock masses through intact material. Thus, failure is not restricted to the joints but, rather, can be developed simultaneously and/or progressively in both intact and joint segments. The random shape of the blocks generated in the modeling approach can allow tensile stresses to arise and produce tensile fracturing throughout the intact material.

This approach is not based on a fracture mechanics approach where fracture propagation is controlled by the fracture toughness and the stress intensity factor at the crack tip. Instead a failure approach is adopted in the UDEC-DM where fracturing occurs when the stress level exceeds the strength in any flaw inside the model. In the present study, the Mohr-Coulomb criterion with a tensile cutoff is used, and the flaws may fail either in shear or in tension.

3. FLAW PATTERNS IN ROCK

In addition to the geomechanical properties of rock mass flaws, the geometrical properties are of great concern in characterizing a rock mass. The blocks in a rock mass are formed by flaws with different patterns formed in nature under different geological circumstances. Understanding the origin of a rock mass would help to have a general idea about the pattern of those flaws. For example, in sedimentary rocks, flaws are generally three perpendicular sets with different degree of persistency. In plutonic rocks, these flaws have an irregular shape that intersect each other at different angles.

Dershowitz and Einstein [12] pointed out that two main approaches have been used to describe the assemblage of geometric flaw characteristics in a rock mass: the disaggregate characterization in which each flaw is described separately, for example, through spacing distribution, and the aggregate characterization in which the interdependence of the flaw characteristics is captured through the formulation of flaw system models. The models can represent real flaw geometries and, as a result, can represent the rock mass geometry. Examples of these flaw model systems are the orthogonal system, which consists of three sets of orthogonal flaws, and the mosaic block tessellation models. According to Ambarcumjan [13] the mosaic tessellation randomly subdivides of the plane into non-overlapping convex polygons. The block shapes can vary and be irregular, and the flaws are the faces of those blocks.
Dershowitz and Einstein [12] stated:

> Since jointing in Mosaic Block Tessellation models is defined by the faces of a process of non-overlapping blocks completely containing the rock mass, they are appropriate for joint systems which are actually the result of a process of block formation in a rock mass. One example of such a joint system is jointing in columnar Basalts. (p. 26).

One of the mosaic block tessellation models is the Voronoi tessellation, which can be utilized in the discrete element modeling approach and used to create realistic rock mass simulation.
Dearman [14] discussed the types of blocks formed in natural rock masses. He stated that flaws' patterns and the difference in spacing and degree of persistency within each flaw set determined the shape of the resulting blocks. For example, these blocks can be described in three dimensions as polyhedral, cubic, etc. (see Figure 4). These examples are few of many patterns that can be encountered in natural rock formations.

4. FAILURE CRITERION OF THE FLAWS

In UDEC, the numerical contacts are of two types: corner-to-corner contacts and edge-to-corner contacts. However, in rocks, edge-to-edge contact is important because it corresponds to the case of a rock joint closed along its entire length. A physical edge-to-edge contact corresponds to a domain with exactly two numerical contacts. The joint is assumed to extend between the two contacts and to be divided in half, with each half-length supporting its own contact stress. Incremental normal and shear displacements are calculated for each point contact and associated length [3].

In the normal direction, the stress-displacement relation is assumed to be linear and controlled by the constant normal stiffness (k_n) such that

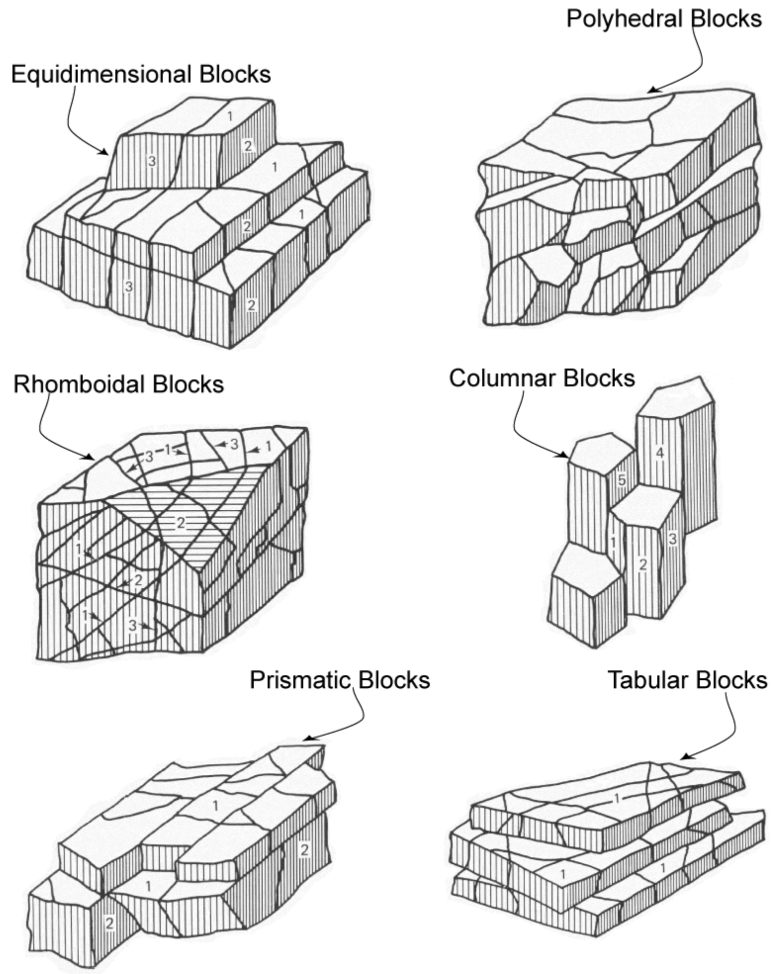

Figure 4: Rock mass block shape, the numbers refers to various flaw sets (modified from Dearman, [14])

$$\Delta\sigma_n = -k_n \Delta u_n, \tag{1}$$

where $\Delta\sigma_n$ is the effective normal stress increment, and Δu_n is the normal displacement increment. There is also a limiting tensile strength, T, for the joint in the normal direction. If the tensile strength is exceeded (if $< -T$), then $\sigma_n = 0$. In the shear direction, the response is governed by constant shear stiffness. The shear stress, τ_s, is controlled by a cohesive (c) and frictional (ϕ) strength according to the Coulomb slip model (Itasca, [3]), such that

$$|\tau_s| \le c + \sigma_n \tan\phi = \tau_{max}; \tag{2}$$

then

$$\Delta\tau_s = -ks\Delta u_s^e ; \tag{3}$$

or else, if

$$|\tau_s| \ge \tau_{max}, \tag{4}$$

then

$$\tau_s = \text{sign}(\Delta u_s)\tau_{max}; \tag{5}$$

where Δu_s^e is the elastic component of the incremental shear displacement, and Δu_s is the total incremental shear displacement (Itasca, [3]).

The basic joint model used in UDEC that captures several of the features in the normal and shear direction is the Coulomb slip model with tension cutoff. The Coulomb slip model is an elastic-perfect plastic model (Figure 5). Notice that in Figure 5, σ_t should be drawn in $\sigma_1 - \sigma_3$ space not shear-normal stress space and this diagram is only for demonstration purpose. The Coulomb model can also be used to approximate a displacement-weakening behaviour by setting the joint cohesion, friction, and tensile strength to reduced values whenever either the tensile or shear strength is exceeded.

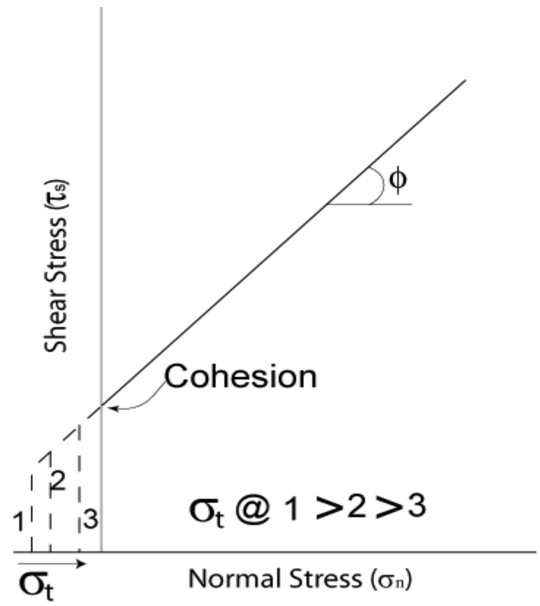

Figure 5: Coulomb-slip model used to simulate the flaws behavior

Lajtai [15] stated that at low normal stress the rock mass strength is totally controlled by the tensile strength (Equation 6). The tensile stresses cause nonlinearity in the failure envelope in the Mohr-Coulomb space. Moreover, Cho et al. [5] found that the formation of the shear zone was preceded by tensile fracturing aligned with the major principal stress direction. In addition, in rock slopes, the majority of the back-calculated cohesion is mostly apparent cohesion due to asperities and interlocking but not true cohesion.

Moreover, Skempton [16] showed that the long term (decades long) stability of slopes in stiff overconsolidated clay was a function of the loss of cohesion with time. In soils, cohesion is a function of Van de Vaals' bonding forces which are influenced by environmental factors such as water content. In many rocks, the cohesive forces are dominated by ionic and covalent bonds, which are not readily susceptible to environmental factors. However, these bonds are weaker in tension than in shear. Hence, if tensile stresses exist, these bonds may break at relatively low stress magnitudes.

Aydin and Basu [17] showed, using Brazilian tensile tests that the tensile strength of a rock is extremely sensitive to the degree of weathering. They found that the tensile strength could decrease by an order of magnitude depending on the extent of weathering, and that the stiffness of the rock decreased as the tensile strength decreased. In other words, weathering may be a significant factor in controlling the behaviour of rock slopes, if the stability of the slope is controlled by the tensile strength. Hence, in this study, the tensile strength of the flaws was decreased gradually to study the effect of tensile strength degradation on rock slopes, while, cohesion and friction angle were kept constant. Figure 5 presents the modeling procedure used in this paper.

$$\tau = \sqrt{\sigma_t(\sigma_t - \sigma_n)}, \tag{6}$$

where σ_t is the tensile strength, and σ_n is the normal stress.

The normal stiffness of the flaws is calculated from Equation 7. At the beginning of each simulation, the shear stiffness is assumed to be equal to the normal stiffness, and then the response of the model is examined. Next, a trial-and-error procedure is adopted to match the deformation of the numerical model with the actual measured deformation, if any. If the measured deformation is not available, the shear stiffness is changed to match the expected behaviour of the model.

According to Itasca [3], up to ten times the normal stiffness calculated from Equation 7 can be assigned to the flaws. If the joint stiffnesses are greater than 10 times the equivalent stiffness, the solution time of the model will be longer than for the case in which the ratio is limited to ten, without a significant change in the behaviour of the model:

$$k_n = \left[\frac{(K+\frac{4}{3}G}{\Delta Z_{min}}\right], \tag{7}$$

where k_n = normal stiffness, K is the bulk modulus, G is the shear modulus, and Z_{min} is the smallest width of an adjoining zone in the normal direction (see Figure 6).

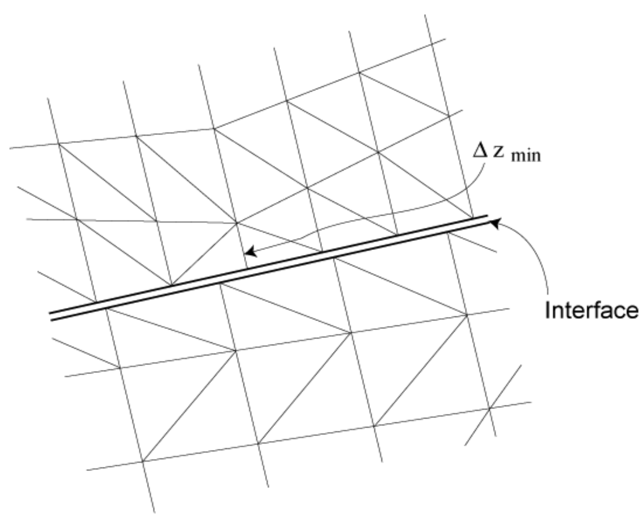

Figure 6: Definition of zone dimension used in stiffness calculation, Equation 7.

Small scale flaws can be very stiff i.e., relative to the size of the model, as the flaws can represent grain-boundary flaws or larger scale internal flaws which have a very small aperture and justify the relatively high normal and shear stiffness used in some models.

5. DAMAGE MODEL ON DIRECT SHEAR TESTS

Lajtai [18] conducted a series of tests using plaster of Paris to simulate intact rock blocks. The blocks, containing rectangular voids to represent the discontinuous nature of the joints, were subjected to direct shear stress at various normal stresses. Lajtai argued that for non-continuous joints, the minor principal stress in the rock bridge is tensile even if the all around stresses are compressive, and that these tensile stresses are responsible for forming the fractures in the rock bridges. Lajtai concluded that at low normal stress, tensile fracturing in the rock bridge was the dominant mode of failure, but that as the normal stress increased, the failure mode progressively became dominated by shear mechanisms.

Based on his finding, Lajtai suggested that the failure of rock containing intact rock bridges between joints could be represented by a nonlinear envelope whose nonlinearity occurred because of the non-uniform mobilization of friction [19]. At low normal stress, the tensile strength controlled the failure while at high normal stress; the frictional strength dominated the failure process.
The properties of the plaster of Paris used by Lajtai [18] were as follows: unconfined compressive strength of 4.1 MPa, a friction angle of 37°, tensile strength of 1.1 MPa, and an estimated cohesion of less than twice the tensile strength. The Mohr-Coulomb failure criterion with tension cutoff was used to control the flaws' behaviour in this modeling approach.

To model the direct shear test, the cohesion, the friction angle and the tensile strength needed to be known prior to conducting the analysis. However, the tensile strength and the friction angle were known while the cohesion was unknown, so the UDEC-DM was utilized to back-calculate the cohesion strength. A two-to-one model was prepared with an edge length of 7 mm, which is the same edge used in the direct shear model. The model was subjected to a constant displacement rate to induce stresses until failure was achieved. The axial stress and vertical strain were monitored by using Fish functions. A trial-and-error study was conducted to match the unconfined compressive strength of 4.1 MPa by varying the cohesion of the flaws while keeping the tensile strength and friction angle constant, Table 1 shows the flaws' properties used in the unconfined compressive strength model. Figure 7(a) shows the stress-strain curve resulting from this test. The failed sample is shown in Figure 7(b).

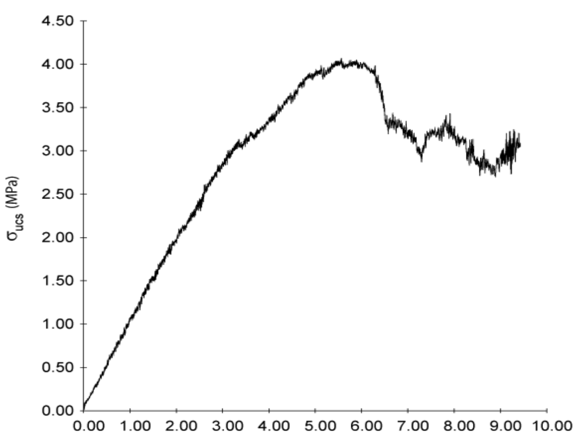

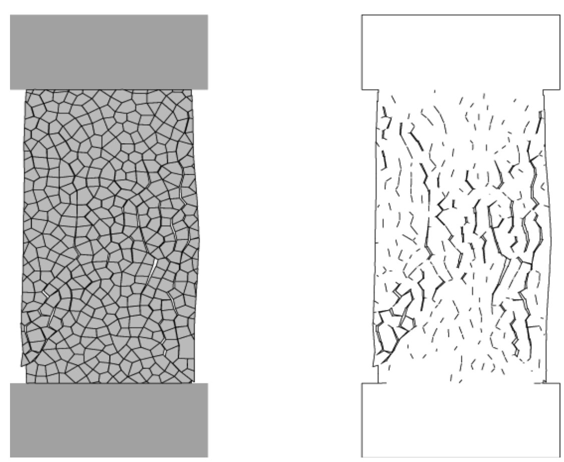

a) Stress-strain response b) Model of intact rock after failure

Figure 7: The unconfined compressive strength of plaster of Paris

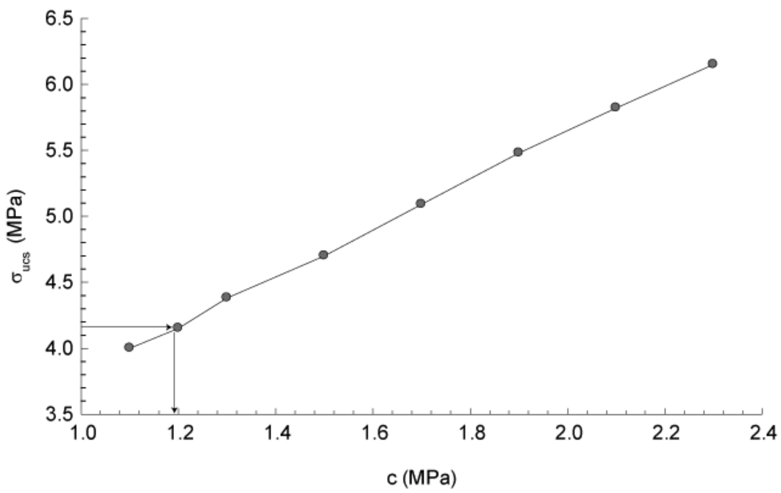

Figure 8: Effect of cohesion strength on the uniaxial strength

Figure 8 shows the variation of the cohesion with the unconfined compressive strength, at cohesion of 1.2 MPa the unconfined compressive strength was approximately equal to the UCS of the laboratory sample. The UDEC-DM model was used to simulate Lajtai's direct shear experiments (Figure 9). The tensile strength of the plaster of Paris was approximately 1.1 MPa, and the friction angle was 37°, these values assigned to the flaws in the model.

The plaster of Paris Young's modulus can range between 2-10 GPa (Vekinis et al., [20]). In this model, the blocks had a Young's modulus of 4.5 GPa. The UDEC-DM model was calibrated to these properties such that the uniaxial compressive strength was captured as mentioned above (Table 1). In these simulations, the flaw size in the plaster of Paris was very small, i.e., sub-mm scale. However, in the UDEC-DM model, the length of the polygonal block was limited to 7.0 mm.

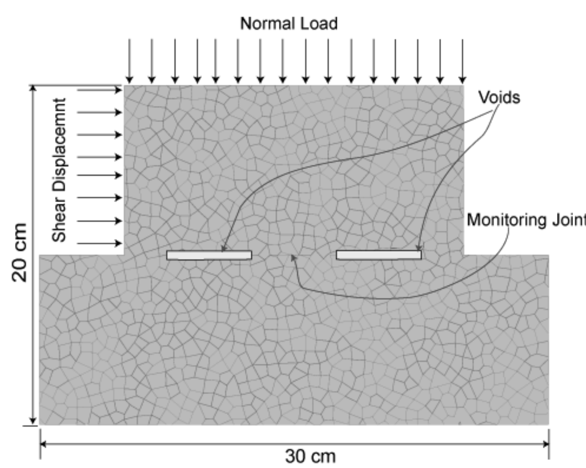

Figure 9: The UDEC-DM model used to simulate Lajtai's direct shear experimental results

Different block lengths were evaluated ranging from 5 mm to 11 mm, and the length used in this study (7 mm) provided a reasonable compromise between accuracy and simulation time. A total of 23 UDEC-DM models were carried out, Figure 10 compares the UDEC-DM model results with those obtained by

Lajtai. These results suggest that this approach is capable of capturing the behaviour of discontinuous rock joints subjected to direct shear and automatically captures the nonlinear failure envelope commonly observed in rock testing. Lajtai [17] also presented a direct shear test results from samples with closed joints.

Table 1: Comparison between Lajtai's plaster of Paris model properties and those used in the UDEC-DM

Properties	UDEC-DM	Lajtai
Friction angle(°)	37	37
ó$_t$(MPa)	1.1	1.1
C(MPa)	1.2	$< 2\sigma_t$
Normal Stiffness (GPa/m)	40	
Shear Stiffness (GPa/m)	20	
Joint aperture (mm)	0.1	

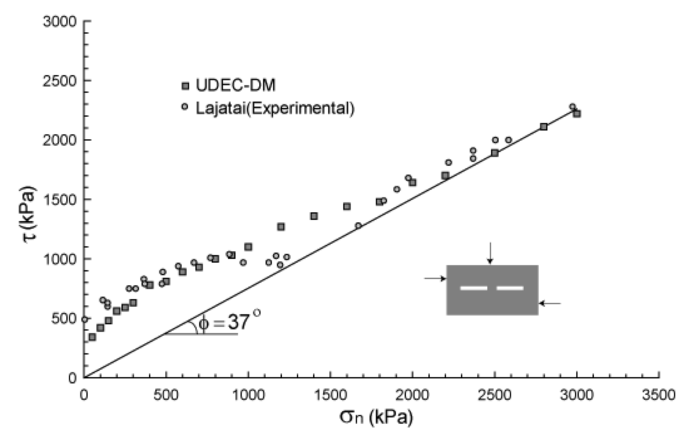

Figure 10: Comparison of UDEC-DM model results with the results from direct shear tests on plaster of Paris and open joints (data from Lajtai, [18])

The direct shear experiment was also modeled numerically by using the UDEC-DM in the same manner for the model with the open joints and the same properties shown in Table 1. A close agreement was achieved between the experimental results and the numerical simulation (see Figure 11). Notice that the direct shear tests were performed under a limited range of normal stress. More data points are needed to explain the small discrepancy between the results in Figure 11; however, the trend of the data is in good agreement. In addition, while the actual friction of the joint is unknown the joints in the numerical model were assigned a friction angle of 30°.

6. THE EFFECT OF DISCONTINUITY PERSISTENCE

The effect of discontinuity persistence has been investigated by using numerical modeling of the direct shear test. The degree of persistence (k) is equal to the ratio between the total lengths of the joint segments to the total length of the model in the direction of shearing. Five models with k = 0, 0.25, 0.5, 0.7 and 1.0 were simulated. Joints were inserted at each side of the model (see Figure 13). A friction angle of 30° was used for both the flaws and the joint segments. The flaws ware assigned a tensile strength of 1.0 MPa, while the tensile strength and the cohesion for the joint segments were equal to zero. Table 1 shows the properties used in this model with a friction angle of 30° for the intact rock and the joints to allow shear failure at low (k). The normal and shear stiffness of the joints were the same as the flaws in table 1.

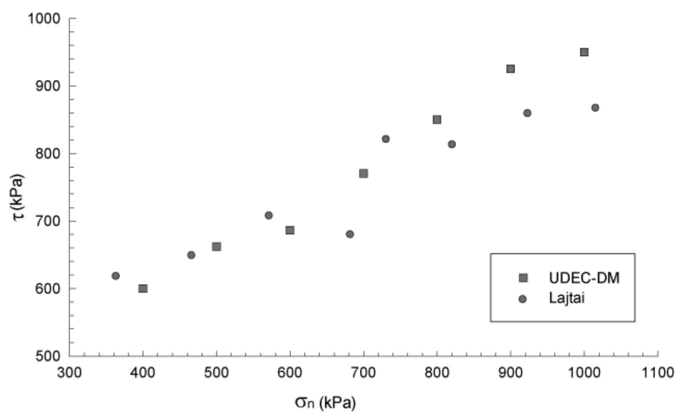

Figure 11: Comparison of UDEC-DM model results with the results from direct shear tests on plaster of Paris and closed joints [18]

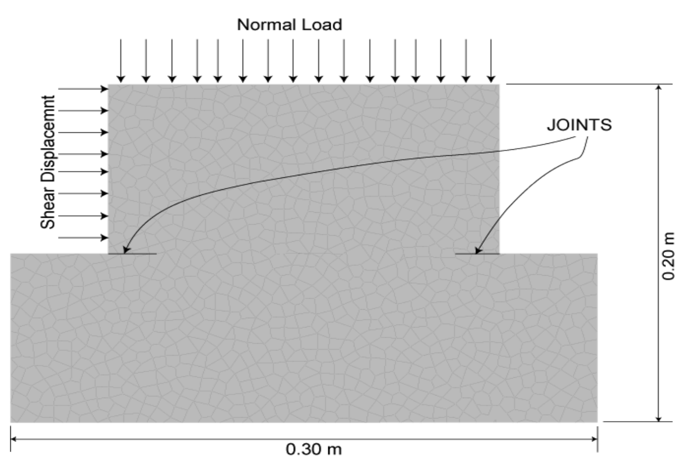

Figure 12: Non-persistent joints direct shear model

Normal stress was applied, and the model was subjected to shear displacement from left to right (see Figure 12). The shear stresses were monitored along the forced shear plane. For each model, the normal stress was varied between 0.3 to 2.4 MPa. Figure 13 shows the failure envelope for the five models. As the length of the joints increased, the rock became weaker in the shear, and the shear strength decreased as a sign of the progressive failure effect due to the presence of the joints. As the normal stress increased the rock mass dilation will be inhibited, in nature the rock mass, the intact material will be sheared off and will not contribute to the total rock mass strength under relatively high normal stress (compared to the UCS) and sliding will occur on the basic friction angle. Moreover, at high value of k (greater than 0.7), the contribution of the intact rock to total strength will be less compared to the contribution at low values of k as shown in Figure 13.

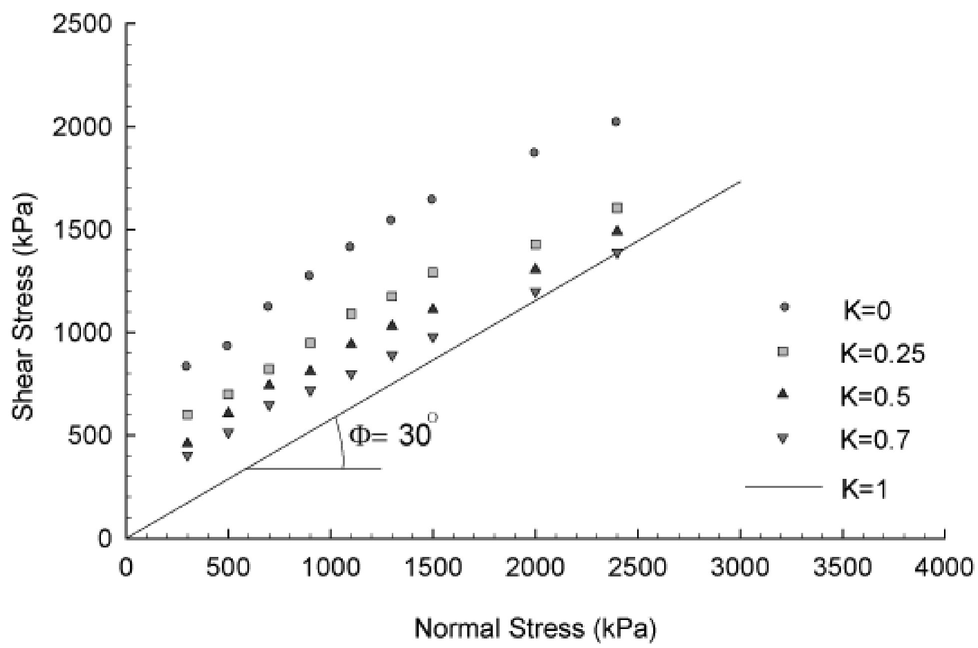

Figure 13: Failure envelope of non-persistence joint direct shear model

If k>0, i.e., if the rock is jointed, the strength of the rock is controlled by both the joints and the intact material. At k=1.0, the strength was totally controlled by the basic friction angle of the rock (30°). As the normal stress increased, the shear strength decreased to the ultimate strength at a normal stress lower for high k than for low k. As the normal stress approached or exceeded the unconfined compressive strength of the rock material, the degree of discontinuity had no effect as the strength of the rock was controlled by the friction angle of the crushed material (the basic friction angle). In order to clarify this point, the shear strength of the jointed models was normalized to the intact material strength derived from the UDEC-DM direct shear model. The results are plotted against the normal stress in Figure 14.

As this figure shows, the difference between the normalized strength and the frictional strength decreased as the normal stress increased, and eventually at high normal stress, the strength of the partially jointed rock (k<1) became equal to the ultimate strength derived from the basic friction angle. These results support the importance of the joints in rock mass analysis, especially in low-stress environments such as those involving slope stability problems. To build a complete geological model for a rock mass, the planes of weakness must be included to contribute to the rock mass's total strength. This modeling approach can explicitly model the joints and allow fractures to initiate and propagate and cause coalescence between the pre-fractured joints. The existence of joints inside the rock mass will introduce weakness planes and reduce the shear strength of the intact rock. The direct shear model using the UDEC-DM provides insights into the effect of the planes of weakness on the rock mass strength envelope and the progressive failure.

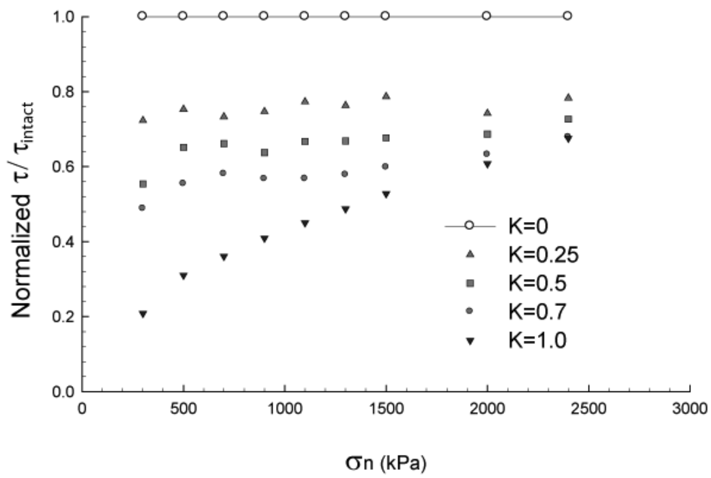

Figure 14: Normalized shear strength of jointed rock to the strength of the intact material

7. EFFECT OF TENSILE STRENGTH IN THE DIRECT SHEAR TEST

The model shown in Figure 12 represents a direct shear test model. If k =0, the direct shear for the intact material is obtained. The advantage of this damage model is that it provides heterogeneity and interlocking inside the rock mass, and the failure path is not predetermined; i.e., the failure can follow any arbitrary path, and the material can also fail in different mechanisms.

To examine the ability of the UDEC-DM to capture the tensile strength in the direct shear model, two models with a friction angle of 30° and tensile strengths of 0.5 MPa and 1.0 MPa were numerically simulated. Nonlinear failure envelopes were obtained by using this modeling approach. Figure 15 shows the failure envelope for both cases. These results indicate that the UDEC-DM captured the nonlinearity in the failure envelope predicted in the experiments and also captured the tensile strength effect as shown in Figure 15. The normal and shear stiffness and the cohesion of the flaws used in this model are shown in Table 1.

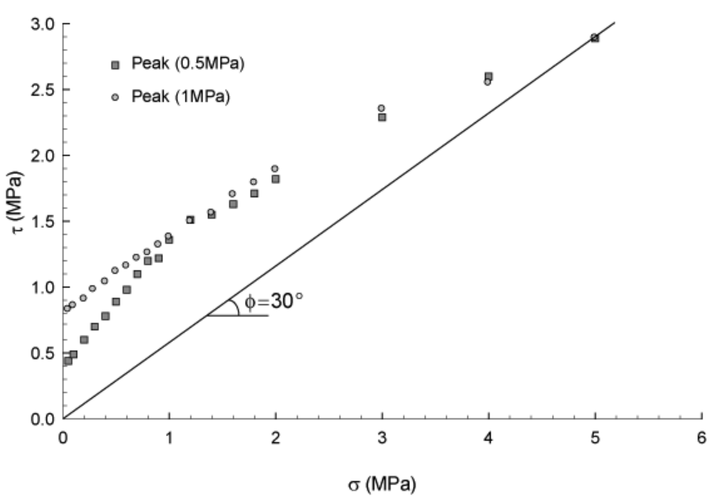

Figure 15: Failure envelope and the tensile strength effect on direct shear discrete element damage model simulation

8. SCALE EFFECT IN UDEC-DM

The effect of edge length scale effect on the UDEC-DM was studied by four models with edge lengths of 0.5, 0.7, 0.9, and 1.1 cm long. The models were similar to the one shown in Figure 12 with no joint segments. The size of the models was kept constant throughout the modeling process. The joint normal and shear stiffness were varied according to Equation 1.7. The models were tested under direct shear loading; a range of normal stress was applied to the model and shearing started. The peak shear stress was monitored and plotted against the applied normal load in Mohr-Coulomb space, (see Figure 16). The results in this direct shear simulation showed that within the range of the edge lengths used in this study, the scale effect was minimal, and the failure envelopes for the four models were reasonably close.

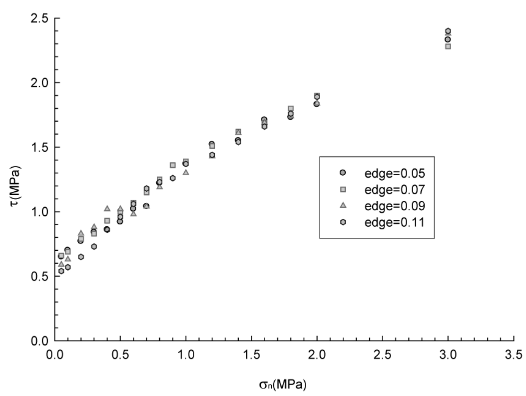

Figure 16: Direct shear results for different edge lengths

9. CONCLUSIONS

Direct shear test was successfully modeled. The discrete element formulation in UDEC was used to create a damage model (UDEC-DM) that can simulate a jointed rock mass and accommodate both continuous and discontinuous joints. The intact rock between the joints are assigned internal flaws and the flaw properties can be adjusted to simulate a rock mass that varies from a strong brittle rock mass to a very weak one. The UDEC-DM showed close agreement with experimental results conducted on plaster of Paris. Numerical modeling was also used to model direct shear tests of discontinuous open and closed joints. The resulting failure envelopes were nonlinear and were found to be in good agreement with experimental results.

10. ACKNOWLEDGMENTS

I would like to thank Dr. Derek Martin and Dr. David Cruden for their advice during this research.

11. REFERENCES

[1] Stead, D., Eberhardt, E., Coggan, J., and Benko, B., (2001). "Advanced numerical techniques in rock slope stability analysis-application and limitations." *In Landslide-Causes, Impacts and countermeasures,* pp. 615-624. Davos, Switzerland.

[2] Cundall, P. A., (1971). "A computer model for simulating progressive large scale movements in blocky rock systems". *In Proceedings of the Symposium of the International Society of Rock Mechanics*, ISRM, pp. 129–136. ISRM, Nancy, France.

[3] Itasca, (2004). "UDEC Universal Distinct Element Code, Version 4.0." Itasca Consulting Group,Inc., Minneapolis.

[4] Pierce, M., Mas Ivars, D., Cundall, P.A. & Potyondy, D.O. (2007). "A synthetic rock mass model for jointed rock." *In Rock Mechanics, Meeting Society's Challenges and demands*, edited by E. Eberhardt, D. Stead, and T. Morrison, vol. 1, pp. 341-349. Vancouver, B.C.

[5] Cho, N., Martin, C., and Sego, D., (2008). "Development of a shear zone in brittle rock subjected to direct shear". *International Journal of Rock Mechanics & Mining Sciences*, doi:10.1016/j.ijrmms.2008.01.019.

[6] Potyondy, D. and Cundall, P., (2004). "A bonded particle model for rock". *International Journal of Rock Mechanics and Mining Sciences and Geomechanics Abstract*, 41: 1329–1364.

[7] Lorig, L. J. and Cundall, P. A., (1987). "Modeling of reinforced concrete using the Distinct Element Method". *In Fracture of Concrete and Rock*, edited by S. B. Shah and S. E. Swartz, pp. 276–287. SEM-RILEM international Conference, Springer Verlag New York Inc., Houston, Texas, USA.

[8] Watson, A., Martin, C., Moore, D., Thomas, W., and Loren, J., (2006). "Integration of geology, monitoring and modelling to assess rockslide risk". *Rock and Soil Engineering*, Felsbau, 3: 50–58

[9] Alzo'ubi, A., Martin, C., and Cruden, D., (2007). "A discrete element damage model for rock slopes". *In Rock Mechanics, Meeting Society's Challenges and demands*, edited by E. Eberhardt, D. Stead, and T. Morrison, vol. 1, pp. 503–510. Vancouver, B.C.

[10] Lorig, L.J., Watson, A., Martin, C.D., Moore, D.P. (2009). "Rockslide run-out prediction from distinct element analysis." *Geomechanics and Geoengineering 4(1): 17-25. doi:10.1080/17486020902767321.*

[11] Alzo'ubi, A, Martin, C.D., Cruden, D.M. (2010). "Influence of tensile strength on toppling failure in centrifuge tests." *International Journal of Rock Mechanics and Mining Sciences 47(1): 974-982.*

[12] Dershowitz, W. and Einstein, H., (1988). "Characterizing rock joint geometry with joint system models". *Rock Mechanics and Rock Engineering*, 21: 21–51.

[13] Ambarcumjan, R. V., (1974). "Convex polygons and random tessellations". *In Stochastic Geometry*, edited by E. Harding and D. Kendall, pp. 176–191. Wiley, New York.

[14] Dearman, W. R., (1991). "Engineering Geological Mapping". Butter worth Heinemann Ltd., Oxford.

[15] Lajtai, E., (1969b). "Shear strength of weakness planes in rock". *International Journal of Rock Mechanics and Mining Science*, 6: 499–515.

[16] Skempton, A., (1964). "Longterm stability of clay slopes". *Geotechnique*, 14: 75–101.

[17] Aydin, A. and Basu, A., (2006). "The use of Brazilian test as a quantitative measure of rock weathering". *Rock Mechanics and Rock Engineering*, 39(1): 77–85.

[18] Lajtai, E., (1969c). "Strength of discontinuous rocks in direct shear". *Geotechnique*, 6: 499–515.

[19] Hajiabdolmajid, V., Kaiser, P., and Martin, C., (2003). "Mobilized strength components in brittle failure of rock". *Geotechnique*, 53: 327–336.

[20] Vekinis, G., Ashby, M. F., and Beaumont, P. W. R., (1993). "Plaster of Paris as a model material for brittle porous solids". *Journal of Material Science*, 28: 3221–7.